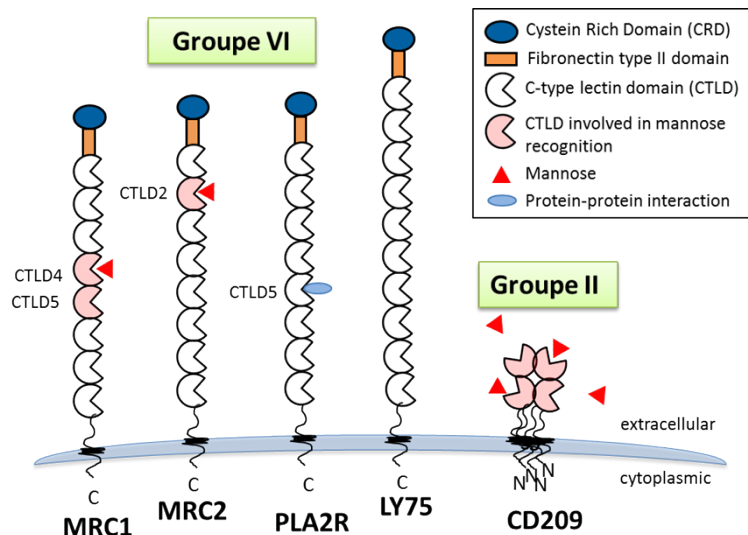


## Supporting Informations

### Identification of MRC2 and CD209 receptors as targets for photodynamic therapy of retinoblastoma using mesoporous silica nanoparticles

A. Gallud,<sup>a</sup> D. Warther,<sup>b</sup> M. Maynadier,<sup>c</sup> M. Sefta,<sup>d</sup> F. Poyer,<sup>e,#</sup> C. D. Thomas,<sup>e,#</sup> C. Rouxel,<sup>f</sup> O. Mongin,<sup>f</sup> M. Blanchard-Desce,<sup>f,#</sup> A. Morère,<sup>a</sup> L. Raehm,<sup>b</sup> P. Maillard,<sup>g,#\*</sup> J.O. Durand,<sup>b,#\*</sup> M. Garcia,<sup>a</sup> and M. Gary-Bobo.<sup>a\*</sup>

Mannose receptors were studied to better understand endocytosis mediated by glycosylated nanoparticles <sup>1, 2</sup>. Macrophage mannose receptor 1 (MRC1), C-type mannose receptor 2 (MRC2), lymphocyte antigen 75 (LY75) and phospholipase A2 receptor (PLA2R) have an overall structural homology but distinct ligand binding profiles <sup>3, 4</sup>. All of them are structurally organized into linear sequence of globular domains to compose a roughly 180 kDa receptor. A cysteine-rich domain is located at the extreme N-terminus, followed by a single fibronectin type-II domain and by eight to ten C-type lectin domains involved in carbohydrate recognition. They also possess a single transmembrane segment, a short cytosolic domain containing motifs able to recognize components of the endocytic pathway <sup>3</sup>. This one allows their recycling between the plasma membrane and the endosomes with a step of 10 rounds each hour in the case of MRC1. Only 10 to 30% of the receptors are recycled to cell surface and the majority resides inside the cell <sup>5</sup>. The potential targeting of CD209 receptor was also investigated. This mannose receptor contains a flexible neck region, a transmembrane region and a cytoplasmic tail that incorporates recycling and internalization motifs <sup>6</sup>. These properties make these lectins interesting for therapeutic targeting.



**Figure S1.** Structure of mannose receptors belong to the C-type lectin receptors family (from <sup>3</sup> with modifications).

### 1. Human and animal rights

The work described was carried out in accordance with The Code of Ethics of the World Medical Association, the French Bioethics Law 2004-800 and the French National Institute of Cancer (INCa) Ethics Charter for experiments involving humans and the EU Directive 2010/63/EU for animal experimentation (authorization no. 91-353).

### 2. Patient Derived Xenograft models

Adult female Swiss nude/nude mice were purchased from Charles River (L'Abresle, France) and bred in the animal facility of Institut Curie. Human tumors provided by the Transfer Department of Institut Curie were initially subcutaneously implanted on the flank of anesthetized nude mice (Isoflurane 2%). Tumors were implanted on flank of mice and were harvested when their size was about 10 mm in diameter.

### 3. Gene expression arrays

RNAs of 37 samples were hybridized to Affymetrix Human Genome U133 plus 2.0 Array Plates (Santa Clara, CA) according to Affymetrix standard protocols. Raw CEL files were RMA <sup>7</sup> using R statistical software and mapped to genes with a Brainarray Custom CDF (EntrezG

version 16.0) <sup>3</sup>. For the public McEvoy et al. dataset <sup>8</sup>, the raw CEL files were downloaded and processed in the exact same manner as the Curie CEL files (Figure S2).

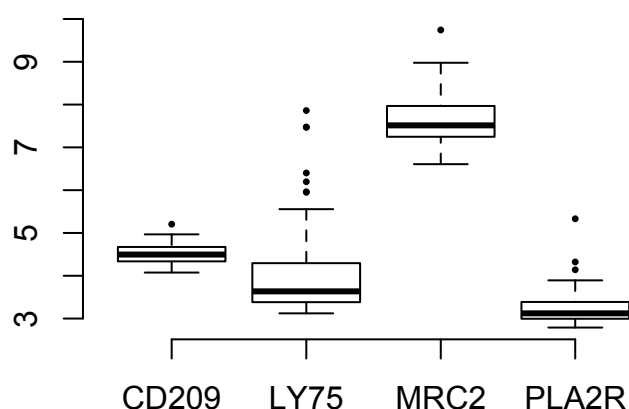


**Figure S2.** Analysis of the publicly available McEvoy dataset gene expression array

#### **4. Synthesis of mesoporous silica nanoparticles MSN-(rho) and MSN-(2hvPS)**

MSN of 200 nm diameter were covalently loaded with rhodamine (rho) or two-photon photosensitizer (2hvPS). Synthesis of **MSN-(2hvPS)** was already described in our previous work <sup>9</sup>, (load of 2hvPS:  $5.8 \times 10^{-3}$  mmol/g<sub>MSN</sub>). Characterization by DLS analysis and TEM microscopy was performed (Figures S3-S4).

#### **MSN-(2hvPS)**

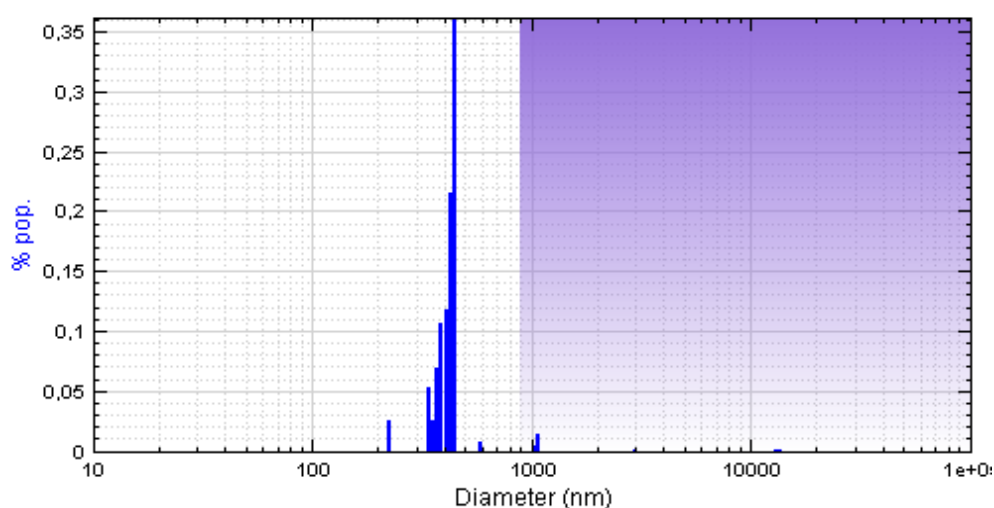


**Figure S3.** Size repartition of MSN-(2hvPS). The DLS measurement in EtOH of the size of the MSN-(rho) shows a narrow distribution around 350 nm.

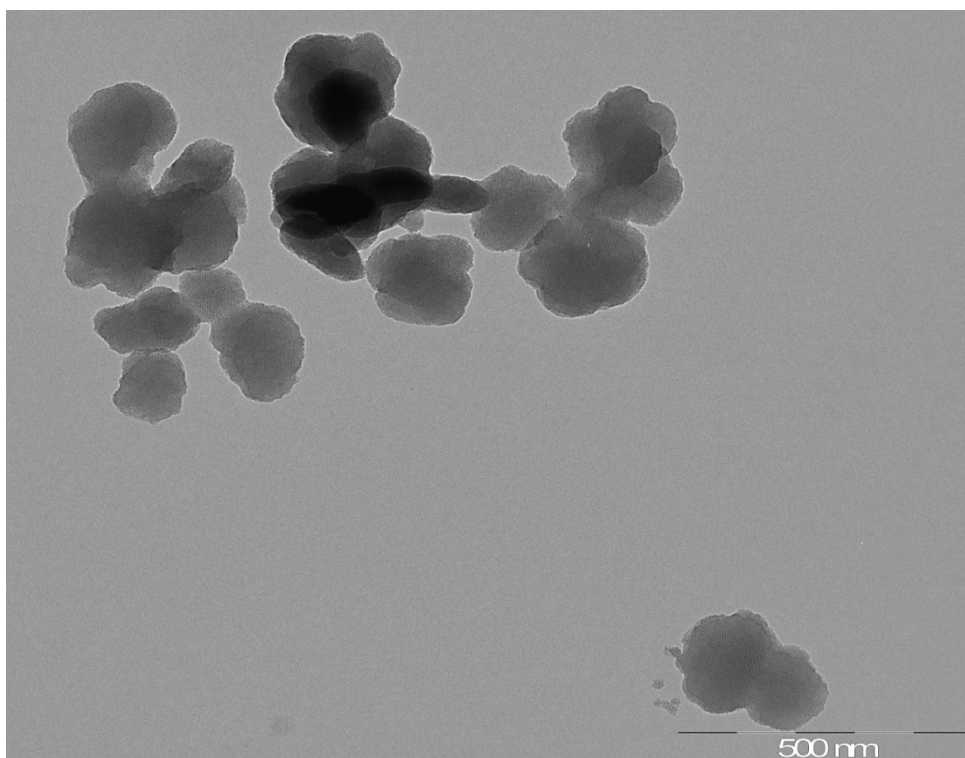


**Figure S4.** TEM image of MSN-(2hvPS).

**a. Synthesis of MSN-(rho)**

30 mg of isothiocyanate rhodamine B ( $5.60 \times 10^{-2}$  mmol ; 1 eq.) were dissolved in 4.36 mL of anhydrous EtOH under argon in a 10 mL round-bottom flask. 13.1  $\mu$ L of aminopropyltriethoxysilane ( $5.60 \times 10^{-2}$  mmol ; 1 eq.) were added. 11.7  $\mu$ L of triethylamine ( $8.4 \times 10^{-2}$  mmol ; 1.5 eq.) were then slowly added and the mixture was stirred for 2 hours at 40°C. After reaction, the solvent and excess of triethylamine were removed under vacuum. The crude product was dissolved in 4.36 mL of EtOH 95% and used without further purification. 686 mg of cetyltrimethylammonium bromide (CTAB) (1.8 mmol) was dissolved in 40 mL of a 0.2 M aqueous sodium hydroxide solution and stirred for 2 hours at 25°C. 1 mL of the previously synthesized solution of rhodamine B trialkoxysilane was added and stirred for 2 minutes. 3.5 mL of tetraethoxysilane ( $1.57 \times 10^{-2}$  mmol) were then added. After 40 sec., 260 mL of deionized water were added. The solution was stirred for 6 min. and quickly neutralised to pH 7 with 0.2 M HCl (about 50 mL). The nanoparticles were recovered through centrifugation (10 min, 20,000 rpm), resuspended in ethanol under ultrasonication and centrifuged. The surfactant was extracted with an ethanolic suspension of  $\text{NH}_4\text{NO}_3$  ( $6 \text{ g}\cdot\text{L}^{-1}$ ).

After centrifugation (10 min, 20,000 rpm), the extraction was repeated twice. The nanoparticles were then washed with water and ethanol, dried under vacuum and stored at  $-20^{\circ}\text{C}$ . Rhodamine :  $1,95 \times 10^{-3}$  mmol/ $\text{g}_{\text{MSN}}$ . Characterization by DLS analysis was performed (Figure S5).

#### b. DLS measurement of MSN-(rho)

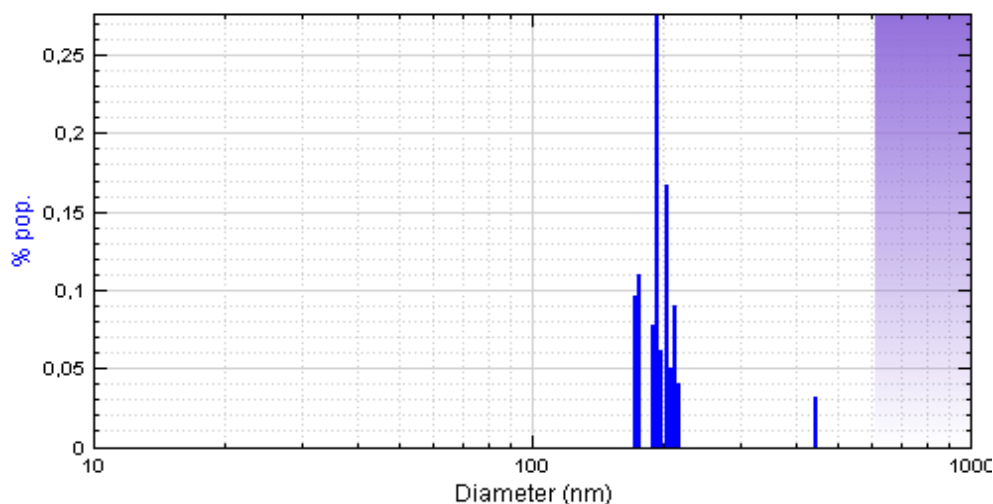


**Figure S5.** Size repartition of MSN-(rho). The DLS measurement in EtOH of the size of the MSN-(rho) shows a narrow distribution around 200 nm.

### 5. Synthesis of MSN-(rho)-NHCO-NHNH<sub>2</sub>

#### a. Boc-hydrazine; Si-C<sub>3</sub>-NHCO-NHNH-Boc (see ESI, Figure S6)

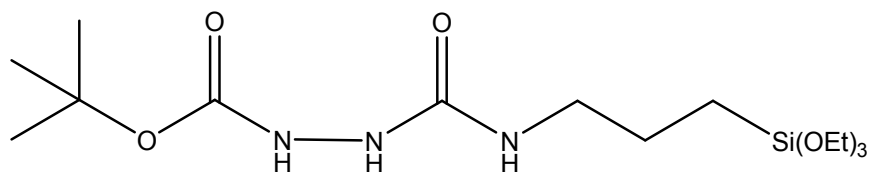


**Figure S6.** Structure of Si-C<sub>3</sub>-NHCO-NHNH-Boc molecule.

2 g of *tert*-butyl carbazate (15.1 mmol ; 1 eq.) were suspended in 100 mL of absolute ethanol. 4.12 mL of isocyanatopropyltriethoxysilane (16.6 mmol ; 1.1 eq.) were then slowly added. The mixture was stirred until the precipitate is fully dissolved. The solvent was then removed under vacuum. The crude product was dissolved in a minimum of boiling  $\text{CH}_2\text{Cl}_2$ . Pentane was then added until a stable precipitate appeared. After one night at  $-20^{\circ}\text{C}$ , the white solid was filtered, washed 3 times with pentane and dried under vacuum (5.20 g ; 13.7

mmol ; yield = 91 %).  $^1\text{H}$  NMR,  $\text{DMSO-}d_6$ , 200 MHz,  $\delta$  (ppm) : 8.43 (s ; 1H) ; 7.49 (s ; 1H) ; 6.23 (s ; 1H) ; 3.70 (q ; J = 6 Hz ; 6H) ; 2.93 (m ; 2H) ; 1.36 (s ; 9H) ; 1.11 (t ; J = 6 Hz ; 9H) ; 0.47 (m ; 2H). Characterization by DLS analysis was performed (Figure S7).

**b. DLS measurement of MSN-(rho)-NHCO-NHNH<sub>2</sub>**

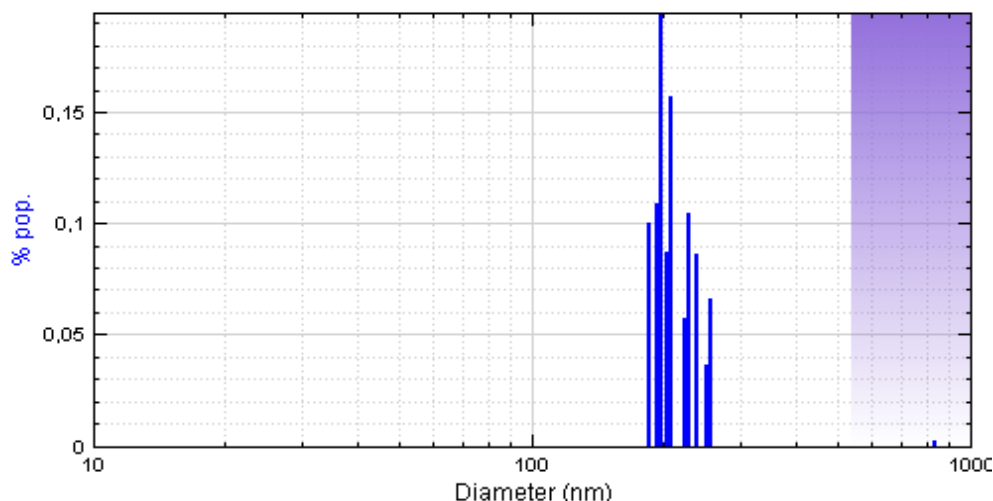


**Figure S7.** Size repartition of MSN-(rho)-NHCO-NHNH<sub>2</sub>. The DSL measurement does not show major increase of the size of the particles after grafting of the semi-carbazide moiety on their surface.

**c. Surface grafting with Boc-hydrazine (MSN-(rho)-NHCO-NHNH-Boc).**

60 mg of 150 nm MSN-(rho) were sonicated in 3 mL of EtOH 95% until they were homogeneously dispersed. 200 mg of Si-C<sub>3</sub>-NHNH-Boc (0.53 mmol) were dissolved in 2 mL of EtOH and then added to the suspension of nanoparticles. The mixture was stirred in dark at 80°C for 4 hours. After reaction, the mixture was cooled to RT. The nanoparticles were centrifugated (10 min, 15,000 rpm) and the pellet was washed three times with EtOH. Elemental analysis: C: 14.53 %; N: 3.96 %. -NHCO-NHNH-Boc:  $9.42 \times 10^{-1} \text{mmol/g}_{\text{MSN}}$  (calculated from analysis)

**d. Removal of the Boc-protecting group (MSN-(rho)-NHCO-NHNH<sub>2</sub>).**

The nanoparticles were resuspended in a mixture of CH<sub>2</sub>Cl<sub>2</sub> and trifluoroacetic acid (1:1 in volume) and sonicated for 5 min. The mixture was then centrifugated (10 min, 15,000 rpm) and the pellet was washed one time with CH<sub>2</sub>Cl<sub>2</sub>, EtOH, water, EtOH and CH<sub>2</sub>Cl<sub>2</sub>. The nanoparticles were then dried under vacuum. Elemental analysis: C: 9.73 %; N: 3.98 %. -NHCO-NHNH<sub>2</sub>:  $9.48 \times 10^{-1} \text{mmol/g}_{\text{MSN}}$  (calculated from analysis).

Surface grafting and removal of the Boc-protective group were analyzed by FTIR by checking the peaks at  $1711.69\text{ cm}^{-1}$  and  $1155.96\text{ cm}^{-1}$  (corresponding to the ester C=O and C-O, respectively) and  $1392.96\text{ cm}^{-1}$  (corresponding to the  $-\text{CH}_3$ ), representing the signature of the Boc-protective group (Figure S8).

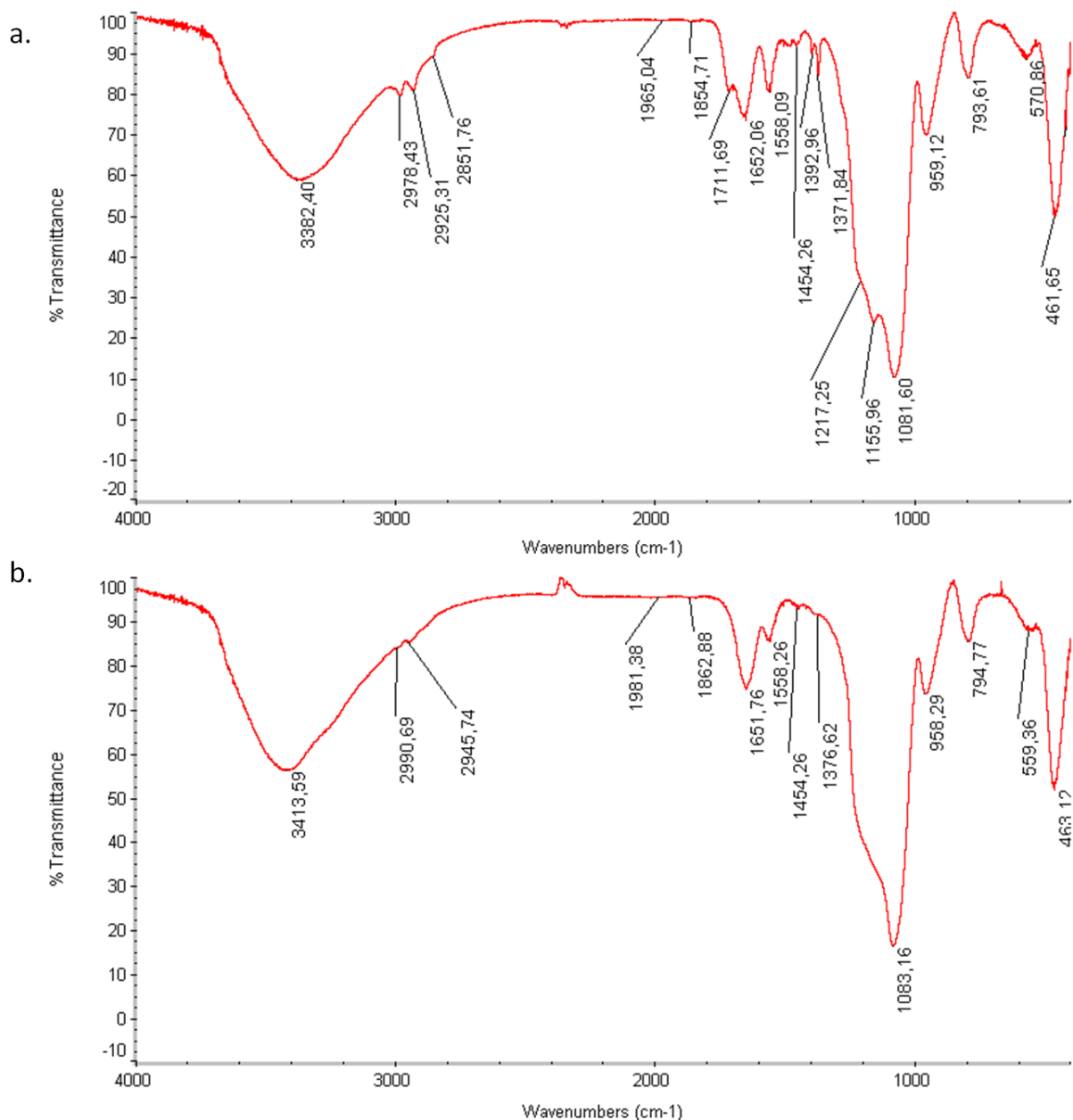


**Figure S8.** FTIR spectra of MSN-(rho)-NHCO-NHNH-Boc (a) and MSN-(rho)-NHCO-NHNH<sub>2</sub> (b). The spectra were taken in KBr pellets and KBr was used as background.

- The peaks at  $1711.69\text{ cm}^{-1}$ ,  $1392.96\text{ cm}^{-1}$  and  $1155.96\text{ cm}^{-1}$  (C=O, C-H and C-O, respectively) show the presence of the Boc-protected semi-carbamide on the surface of the MSN.
- The disappearance of the three previous peaks shows the removal of the Boc-protective group on the MSN.

## 6. Synthesis of MSN-(2hvPS)-NHCO-NHNH<sub>2</sub>

a. Si-C3-NHNH-Fmoc. 10-Oxa-2,3,5-triaza-9-siladodecanoic acid, 9,9-diethoxy-4-oxo-, 9H-fluoren-9-ylmethyl ester. (Figure S9)

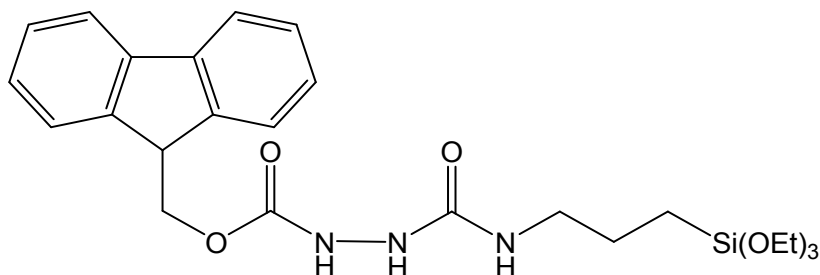


**Figure S9.** Structure of Si-C3-NHNH-Fmoc molecule.

2 g of fluorenylmethyl carbazate (7.87 mmol ; 1 eq.) were suspended in 40 mL of absolute EtOH. 2.16 mL of 3-(triethoxysilyl)propylisocyanate (8.66 mmol ; 1.1 eq.) were added to the suspension. The mixture was gently stirred at RT until the precipitate had totally disappeared. After reaction, the solvent was removed under vacuum. The crude product was dissolved in a minimum of CH<sub>2</sub>Cl<sub>2</sub>. Pentane was then added and the mixture was maintained at 0°C for 2 h for extensive precipitation. The precipitate was filtered and washed three times with pentane. The product was dried under vacuum (3.90 g ; quantitative). <sup>1</sup>H NMR, DMSO-d<sub>6</sub>, 200 MHz, δ (ppm) : 8.99 (s ; 1H) ; 7.89 (d ; J = 8 Hz ; 2H) ; 7.72 (d ; J = 8 Hz ; 2H) ; 7.46-7.23 (m ; 4H) ; 6.33 (s ; 1H) ; 4.29 (m ; 3H) ; 3.72 (q ; J = 6 Hz ; 6H) ; 2.96 (s ; 2H) ; 1.43 (m ; 2H) ; 1.10 (t ; J = 6 Hz ; 9H) ; 0.51 (t ; J = 8 Hz ; 2H).

b. Surface grafting with Si-C3-NHCO-NHNH-Fmoc (MSN-(2hvPS)-NHCO-NHNH-Fmoc).

60 mg of 150 nm nanoparticles were sonicated in 3 mL of EtOH 95% until they were homogeneously dispersed. 200 mg of Si-C3-NHNH-Fmoc (0.40 mmol) were dissolved in 2 mL of EtOH and then added to the suspension of nanoparticles **MSN-(2hvPS)**. The mixture was stirred in the dark at 80°C for 4 h. After reaction, the mixture was cooled to RT. The nanoparticles were centrifugated (10 min, 15,000 rpm) and the pellet was washed three times with EtOH. The grafted nanoparticles were then suspended in 5 mL of a mixture of DMF and piperidine (volume ratio 1:1). The mixture was stirred in the dark for 30 min and then centrifugated (10 min, 15,000 rpm). The supernatant was collected for grafting quantification. The pellet was washed twice with a mixture of DMF and piperidine (volume



ratio 1:1) and three times with EtOH. The particles were dried under vacuum and stored at -20°C. The removal of the Fmoc-protective group was followed by UV absorption analysis and the amount of grafted semi-carbazide on the surface of the nanoparticles was determined by UV quantification and TEM microscopy was performed (Figures S10-S11).

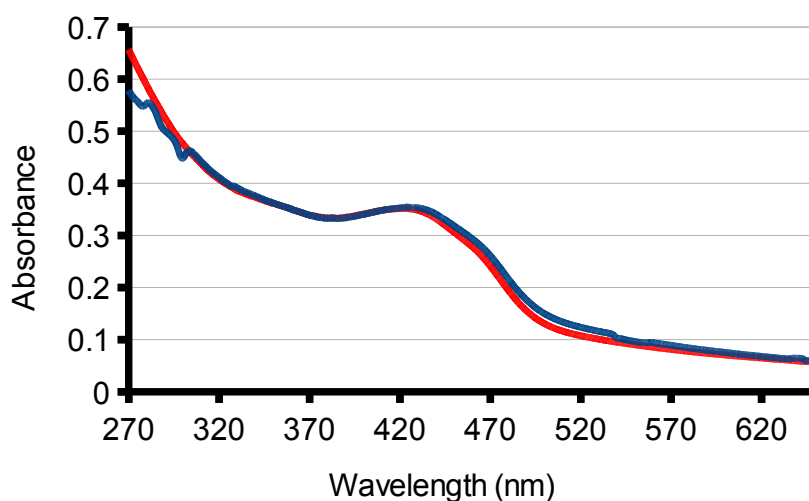


**Figure S10.** UV spectra of MSN-(2hvPS)-NHCO-NHNH-Fmoc (blue line) and MSN-(2hvPS)-NHCO-NHNH<sub>2</sub> (red line). The particles were suspended in ethanol. The disappearance of the typical sharp peak of the fluorine moiety at 301 nm after the deprotection step shows the effective removal of the Fmoc-protective group from the MSN.

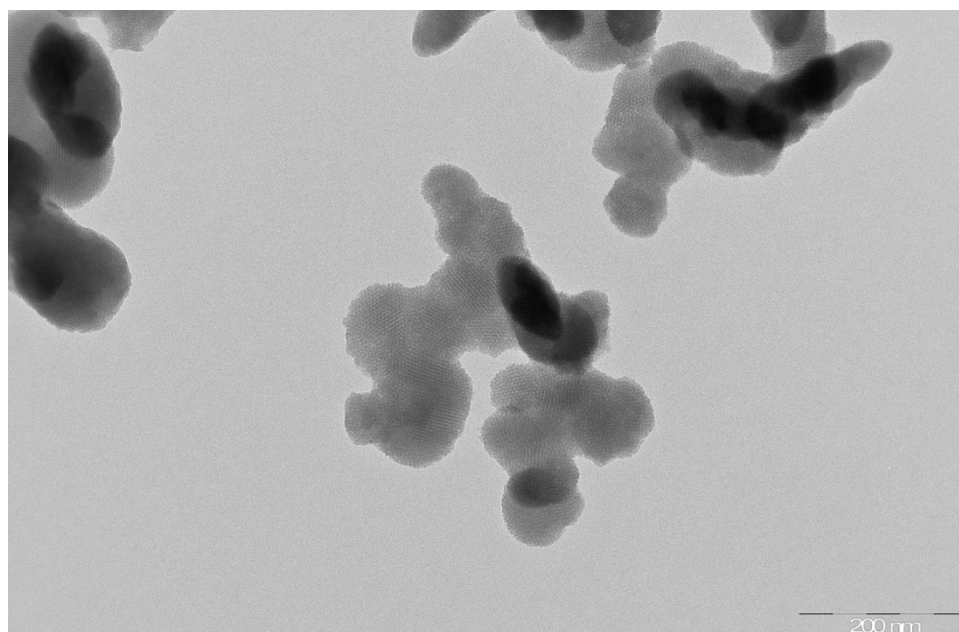


**Figure S11.** TEM image of MSN-(2hvPS)-NHCO-NHNH<sub>2</sub>.

## 7. Coupling of MSN-(rho)-NHCO-NHNH<sub>2</sub> and MSN-(2hvPS)-NHCO-NHNH<sub>2</sub> with antibodies

### a. Oxidation of antibodies

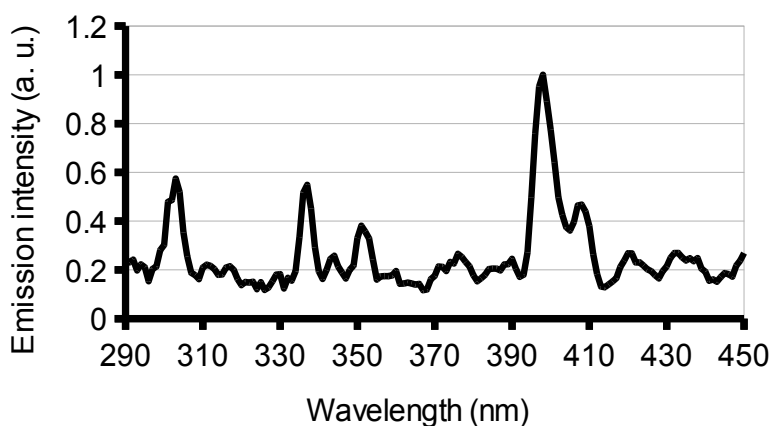
20  $\mu\text{L}$  of a commercial solution of antibody anti-IgGRb (Dako), anti-CD209 (Abnova) or anti-MRC2 (Abcam) at  $1 \text{ mg}\cdot\text{mL}^{-1}$  were diluted in 0.4 mL of phosphate buffer  $\text{Na}_2\text{HPO}_4$  0.01 M (pH 7.4). 10  $\mu\text{L}$  of a 0.1 M aqueous solution of  $\text{NaIO}_4$  were added and the mixture was stirred for 1 h in the dark at RT. The oxidant was then removed by desalting on a Sephadex G25 column. The mixture was eluted with 2000  $\mu\text{L}$  of phosphate buffer  $\text{Na}_2\text{HPO}_4$  0.1 M (pH 7.4). 10 fractions of 200  $\mu\text{L}$  were collected and the presence of the antibodies was determined by UV analysis (absorbance  $\lambda_{\text{max}} = 280 \text{ nm}$ ) or fluorescence ( $\lambda_{\text{ex}} = 270 \text{ nm}$  ;  $\lambda_{\text{em}} = 320\text{-}360 \text{ nm}$ ) measurements. The fractions containing the antibody were gathered.

### b. Coupling with nanoparticles

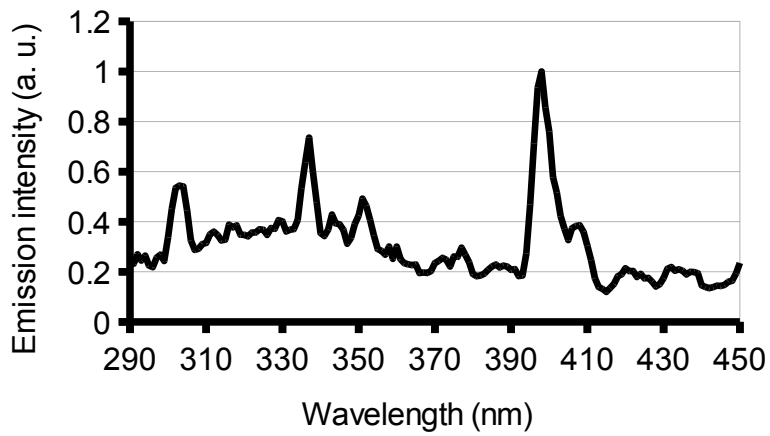
The nanoparticles **MSN-(rho)-NHCO-NHNH<sub>2</sub>** and **MSN-(2hvPS)-NHCO-NHNH<sub>2</sub>** were suspended into phosphate buffer  $\text{Na}_2\text{HPO}_4$  0.1 M (pH 7.4) at a concentration of  $1 \text{ mg}\cdot\text{mL}^{-1}$ . 200  $\mu\text{L}$  of the suspension were added to antibodies containing solutions. The mixture was stirred for 1 h at RT in the dark and was then centrifuged at 15,000 rpm for 10 min. The pellet was washed 3 times with water and stored in PBS. The different supernatants were collected and stored for analysis. The coupling was analyzed by fluorescence measurements of the suspension of nanoparticles in PBS,  $\lambda_{\text{ex}} = 270 \text{ nm}$  ;  $\lambda_{\text{em}} = 320\text{-}360 \text{ nm}$  (Figures S12-S18)

### c. Antibodies grafting: fluorescence measurements

a.



b.



c.

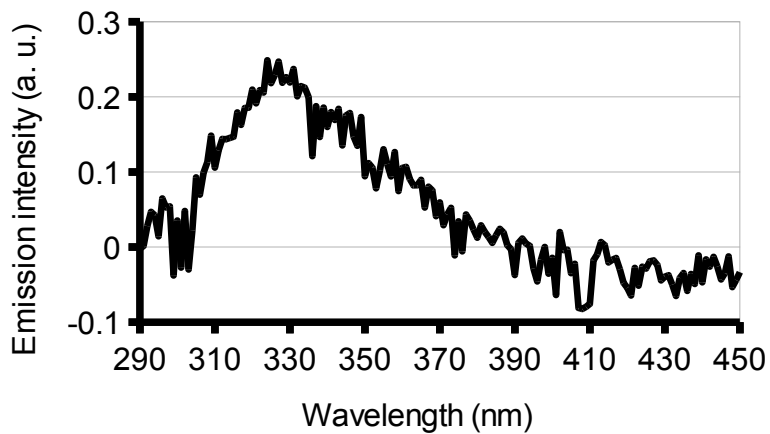


**Figure S12.** Fluorescence spectra of MSN-(rho)-NHCO-NH<sub>2</sub> (a.) and MSN-(rho)-IgGRb (b. and c.).

- Fluorescence spectrum of MSN-(rho)-NHCO-NH<sub>2</sub> corrected versus buffer.
- Fluorescence spectrum of MSN-(rho)-IgGRb corrected versus buffer.
- Fluorescence spectrum of MSN-(rho)-IgGRb corrected versus buffer and (a). (spectrum b. minus spectrum a.)

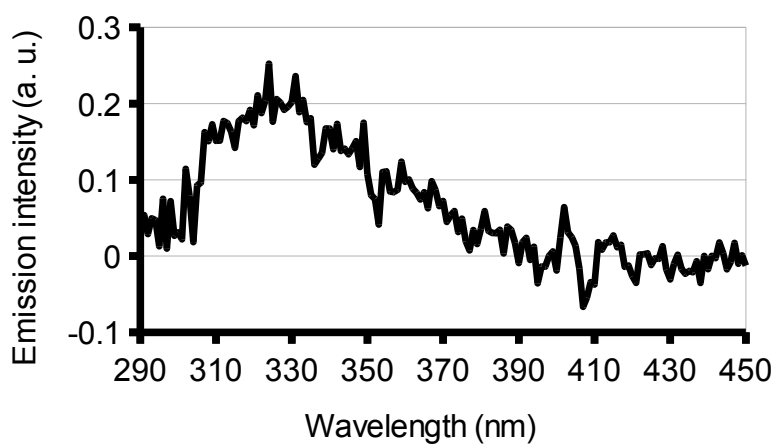


**Figure S13.** Fluorescence spectrum of MSN-(rho)-CD209 (corrected versus buffer and MSN-(rho)-NHCO-NHNH<sub>2</sub>).

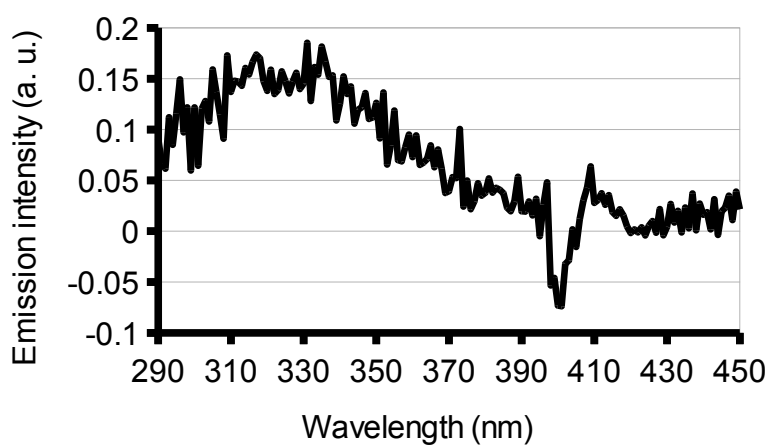


**Figure S14.** Fluorescence spectrum of MSN-(rho)-MRC2 (corrected versus buffer and MSN-(rho)-NHCO-NHNH<sub>2</sub>).

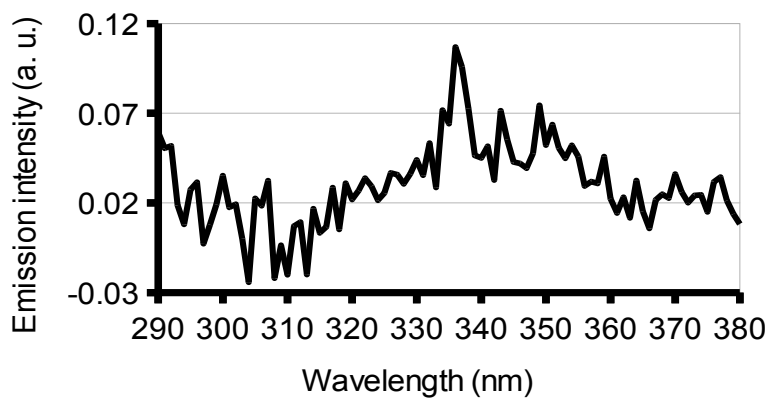


**Figure S15.** Fluorescence spectrum of MSN-(2hvPS)-MRC2 (corrected versus buffer and MSN-(2hvPS)-NHCO-NHNH<sub>2</sub>).

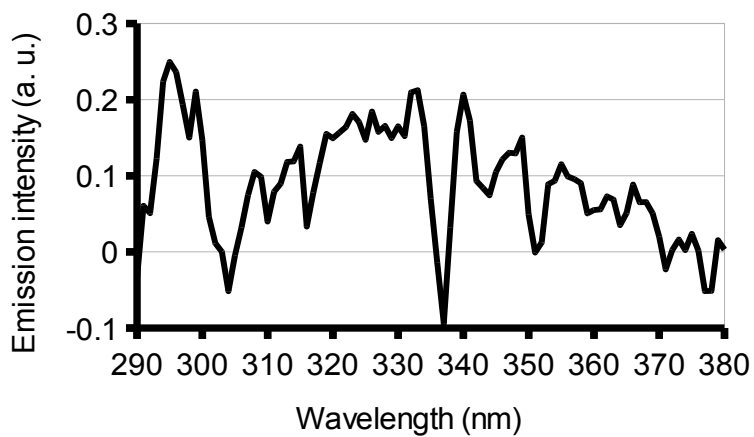


**Figure S16.** Fluorescence spectrum of MSN-(2hvPS)-CD209 (corrected versus buffer and MSN-(2hvPS)-NHCO-NHNH<sub>2</sub>).

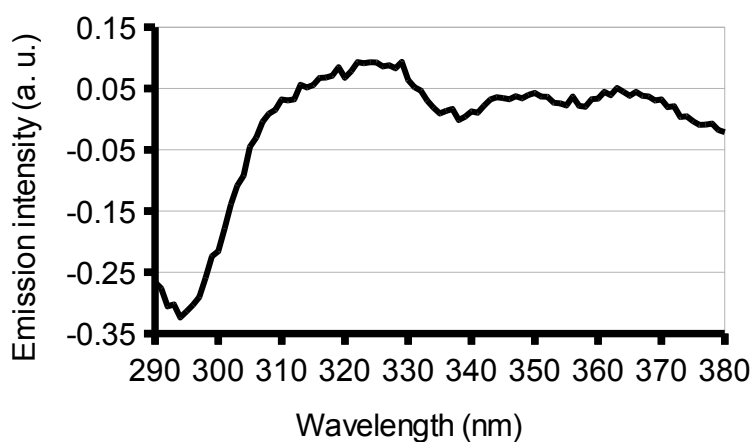


**Figure S17.** Fluorescence spectrum of MSN-(2hvPS)-(CD209+MRC2) (corrected versus buffer and MSN-(2hvPS)-NHCO-NHNH<sub>2</sub>).

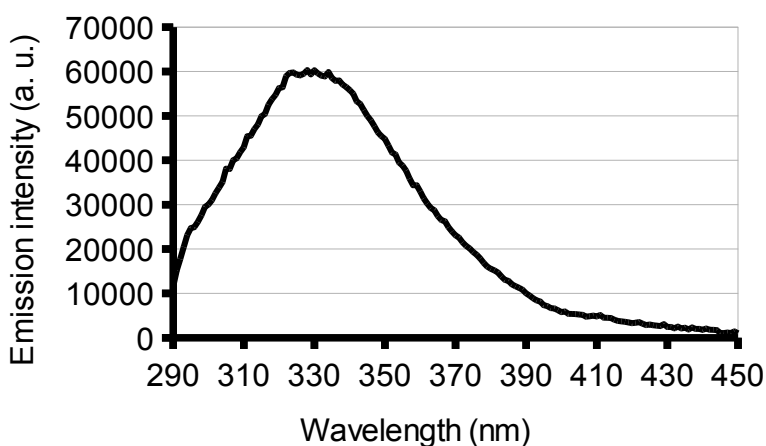


**Figure S18.** Fluorescence spectrum of IgGRb antibodies.

#### d. Grafting quantification

The amount of grafted semi-carbazide on the surface of the nanoparticles was determined by UV-visible quantification of the piperidine-dibenzofulvene adduct formed during the deprotection step ( $\epsilon = 6500 \text{ mol}^{-1} \cdot \text{cm}^{-1}$  at 301 nm in piperidine/DMF 1:1 in volume).

Dilutions of the supernatant were prepared (1; 1/2; 1/5; 1/10). The absorbances of the dilutions were recorded at 301 nm and the concentration of piperidine-dibenzofulvene was calculated as following for each dilution:

$$\text{concentration} = \frac{\text{absorbance}}{\hat{l}_{\mu}(301 \text{ nm})}$$

The calculated concentrations were then corrected regarding the dilution and a mean concentration of the supernatant was determined.

Semi-carbazide concentration:  $3.32 \times 10^{-2} \text{ mmol/g}_{\text{MSN}}$ .

#### e. Spectra analysis

The fluorescence spectra for **MSN-(rho)-IgGRb**, **MSN-(rho)-CD209**, **MSN-(rho)-MRC2**, **MSN-(2hvPS)-CD209**, **MSN-(2hvPS)-MRC2** and **MSN-(2hvPS)-(CD209+MRC2)** and for each supernatant were corrected by subtraction of the buffer spectrum and by a second subtraction with the spectrum of the uncoupled nanoparticles.

## 8. Western blot experiments performed on different cancer cell line

### a. Cell culture conditions

All human cell lines were purchased from ATCC®. Colon carcinoma cells (HCT-116) were maintained in Mac Coy's medium supplemented with 10% fetal calf serum (FCS) and 50  $\mu\text{g}\cdot\text{mL}^{-1}$  gentamicin. Prostatic carcinoma cells (LNCaP) were cultured in RPMI-1640 medium supplemented with 10% FCS, 100 IU penicillin and 100  $\mu\text{g}\cdot\text{mL}^{-1}$  streptomycin, 1% sodium pyruvate, 1% HEPES and 1% glucose. Breast cancer (MCF-7 and MDA-MB-231) and osteosarcoma (Saos-2) cell lines were maintained in DMEM supplemented with 10% FCS and 50  $\mu\text{g}\cdot\text{mL}^{-1}$  gentamicin. All cells grew in humidified atmosphere at 37°C under 5% CO<sub>2</sub>.

### b. Western Blot analysis

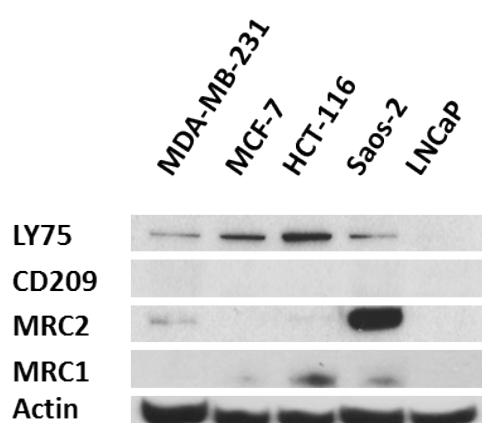


**Figure S19.** Western blot profile of mannose receptors on breast cancer (MDA-MB-231 and MCF-7), colon carcinoma (HCT-116), osteosarcoma (Saos-2) and prostate cancer (LNCaP) cell lines.

## 9. MSN-nanosafety validation

Experiments were performed on Y-79 and WERI-Rb1 retinoblastoma cell lines incubated 72 h with 40  $\mu\text{g}\cdot\text{mL}^{-1}$  of nanoparticles. Data show the absence of toxicity due to the nanoparticles at the concentration used.

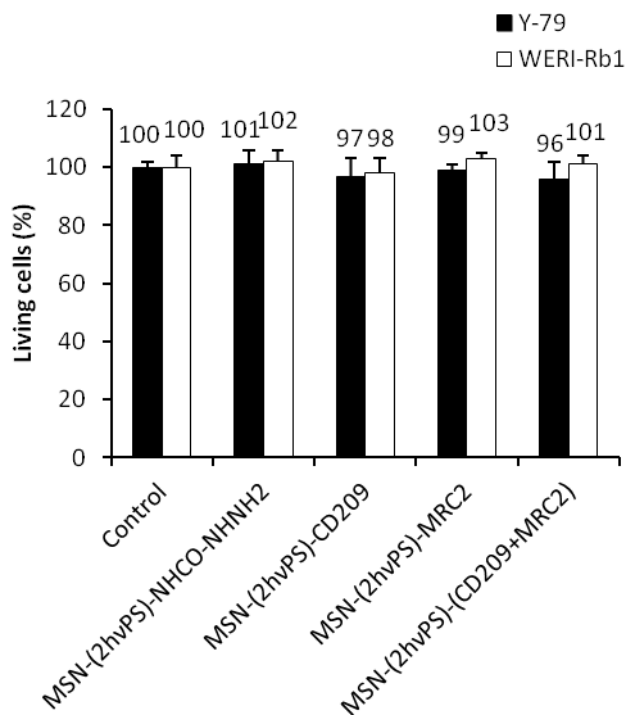


**Figure S20.** Safety of MSNs on Y-79 and WERI-Rb1 retinoblastoma cells without laser irradiation. Cells were incubated with MSNs at  $40 \mu\text{g}\cdot\text{mL}^{-1}$  and MTS cell viability assay was performed 72 h after treatment.

## 10. Reference

1. A. Gallud, A. Da Silva, M. Maynadier, I. Basile, S. Fontanel, C. Lemaire, P. Maillard, M. Blanchard-Desce, O. Mongin, A. Morere, L. Raehm, J. O. Durand, M. Garcia and M. Gary-Bobo, *Journal of Clinical and Experimental Ophthalmology*, 2013, **4**, 4-8.
2. M. Gary-Bobo, Y. Mir, C. Rouxel, D. Brevet, O. Hocine, M. Maynadier, A. Gallud, A. Da Silva, O. Mongin, M. Blanchard-Desce, S. Richeter, B. Looock, P. Maillard, A. Morere, M. Garcia, L. Raehm and J. O. Durand, *Int J Pharm*, 2012, **432**, 99-104.
3. L. East and C. M. Isacke, *Biochim Biophys Acta*, 2002, **1572**, 364-386.
4. J. M. Rini, *Annu Rev Biophys Biomol Struct*, 1995, **24**, 551-577.
5. O. Llorca, *Cell Mol Life Sci*, 2008, **65**, 1302-1310.
6. B. Lepenies, J. Lee and S. Sonkaria, *Adv Drug Deliv Rev*, 2013, **65**, 1271-1281.
7. P. Y. Zhuang, M. J. Zhu, J. D. Wang, X. P. Zhou, Z. W. Quan and J. Shen, *J Dig Dis*, 2013, **14**, 45-50.
8. J. McEvoy, J. Flores-Otero, J. Zhang, K. Nemeth, R. Brennan, C. Bradley, F. Krafcik, C. Rodriguez-Galindo, M. Wilson, S. Xiong, G. Lozano, J. Sage, L. Fu, L. Louhibi, J. Trimarchi, A. Pani, R. Smeyne, D. Johnson and M. A. Dyer, *Cancer Cell*, 2011, **20**, 260-275.
9. M. Gary-Bobo, Y. Mir, C. Rouxel, D. Brevet, I. Basile, M. Maynadier, O. Vaillant, O. Mongin, M. Blanchard-Desce, A. Morere, M. Garcia, J. O. Durand and L. Raehm, *Angew Chem Int Ed Engl*, 2011, **50**, 11425-11429.